Published for SISSA by Springer

Received: *August 24, 2011*
Accepted: *August 25, 2011*
Published: *September 6, 2011*

# Erratum 2: supersymmetric monojets at the Large Hadron Collider

**Benjamin C. Allanach,**[a] **Sebastian Grab**[b] **and Howard E. Haber**[b]

[a] *DAMTP, CMS, University of Cambridge, Wilberforce Road, Cambridge, CB3 0WA, U.K.*
[b] *Department of Physics and SCIPP, University of California, 1156 High Street, Santa Cruz, CA 95064, U.S.A.*

*E-mail:* b.c.allanach@damtp.cam.ac.uk, sgrab@scipp.ucsc.edu, haber@scipp.ucsc.edu

Erratum to: JHEP01(2011)138

Abstract: Supersymmetric monojets may be produced at the Large Hadron Collider by the process $qg \to \widetilde{q}\widetilde{\chi}_1^0 \to q\widetilde{\chi}_1^0\widetilde{\chi}_1^0$, leading to a jet recoiling against missing transverse momentum. We discuss the feasibility and utility of the supersymmetric monojet signal. In particular, we examine the possible precision with which one can ascertain the $\widetilde{\chi}_1^0\widetilde{q}q$ coupling via the rate for monojet events. Such a coupling contains information on the composition of the $\widetilde{\chi}_1^0$ and helps bound dark matter direct detection cross-sections and the dark matter relic density of the $\widetilde{\chi}_1^0$. It also provides a check of the supersymmetric relation between gauge couplings and gaugino-quark-squark couplings.

Keywords: Supersymmetry Phenomenology

Open Access

doi:10.1007/JHEP09(2011)027

JHEP09(2011)027

## Contents



In the appendix of the original publication of this manuscript, we incorrectly identified the variable $t$ of the $2 \to 2$ scattering process with the variable $t_1$ of the $2 \to 3$ scattering process. As a result, the formula that was derived for $d\sigma/dp_T$ was incorrect when the squared matrix element $C_1(s,t)$ of the $2 \to 2$ process depends on $t$. In the new version of the appendix, we derive the correct formula for $d\sigma/dp_T$, which is now a double integral over the energy and the helicity angle of the outgoing jet. Figure 10 shows the unnormalized $p_T$ distribution obtained with the corrected formula for $d\sigma/dp_T$. Remarkably, the resulting figure is almost identical to the one that appears in the original publication. The analytic formulae of the appendix serve as checks of the numerical results obtained in the body of this paper; the latter are not affected by these errata.

## A The Jacobian peak in the transverse momentum distribution

The Jacobian peak is a well-known feature of the transverse momentum distribution of the electron in the process $A+B \to W^{\pm}+X \to e^{\pm}+\nu+X$, where $A$ and $B$ are the initial state hadrons. The resulting peak at $p_T \simeq \frac{1}{2}m_W$ is a consequence of the Jacobian that arises from changing kinematic variables from $\cos\theta$ (where $\theta$ is the center-of-mass scattering angle) to $p_T$.[10] In this paper, we have focused on monojets that arise from $\widetilde{q}\widetilde{\chi}_1^0$ production, where $\widetilde{q} \to q\widetilde{\chi}_1^0$, and the quark is observed as a hadronic jet. The $p_T$ distribution of the quark jet also exhibits a Jacobian peak. In this appendix, we derive an approximate expression for the location of the peak in the transverse momentum distribution of the jet.

Consider the $2 \to 3$ scattering process, which schematically is of the form:

$$a + b \to c + 3\,, \text{ followed by } \quad c \to 1 + 2\,, \tag{A.1}$$

where the decaying particle $c$ is spinless. Since the particles $a$, $b$ and 1 represent light quarks or gluons, we shall set their masses to zero, $m_a = m_b = m_1 = 0$. We denote the mass of particle $c$ (identified as the $\widetilde{q}$) to be $m_c \equiv M$, and the masses of particles 2 and 3 (which are identified with $\widetilde{\chi}_1^0$) to be $m_2 = m_3 \equiv m$.

If the particle $c$ is on-shell, then the corresponding matrix element for the $2 \to 2$ process, $a + b \to c + 3$ is of the form

$$\mathcal{M}(a + b \to c + 3) = C_1(s,t)\,, \tag{A.2}$$

where $C_1(s,t)$ is a dimensionless function of $s \equiv (p_a + p_b)^2$, $t \equiv (p_a - p_c)^2$ and the particle masses. The kinematical limits of $t$ are:

$$-\frac{1}{2}\left[s - M^2 - m^2 + \lambda^{1/2}(s, M^2, m^2)\right] \leq t \leq -\frac{1}{2}\left[s - M^2 - m^2 - \lambda^{1/2}(s, M^2, m^2)\right]\,, \tag{A.3}$$

[10] For a pedagogical treatment, see ref. [103].



JHEP09(2011)027

where

$$\lambda(a,b,c) \equiv a^2 + b^2 + c^2 - 2ab - 2ac - 2bc \tag{A.4}$$

is the well-known triangle function of relativistic kinematics. The squared matrix element for the decay of particle $c$ (which is either $\widetilde{q}_L$ or $\widetilde{q}_R$), summed over final spins, is given by

$$|\mathcal{M}(c \to 1+2)|^2 = C_2(M^2 - m^2)\,, \tag{A.5}$$

where $C_2$ is a dimensionless (real positive) constant that will eventually cancel out in our computation. Using, eq. (A.5) it follows that the total width of particle $c$ times the branching ratio is given by

$$B\Gamma = \frac{C_2 M}{16\pi}\left(1 - \frac{m^2}{M^2}\right)^2\,, \tag{A.6}$$

where the branching ratio $B \equiv B(c \to 1+2)$.

To set up our computation, we work in the center-of-mass system. Then, the four-vectors of the initial states and the observed final state (particle 1) are:

$$p_a = \frac{1}{2}\sqrt{s}(1\,;\,0\,,\,0\,,\,1)\,, \tag{A.7}$$

$$p_b = \frac{1}{2}\sqrt{s}(1\,;\,0\,,\,0\,,\,-1)\,, \tag{A.8}$$

$$p_1 = E_1(1\,;\,\sin\theta\,,\,0\,,\,\cos\theta)\,, \tag{A.9}$$

where $\theta$ is the scattering angle in the center-of-mass frame. Following ref. [104], we define four Lorentz-invariant quantities,

$$t_1 \equiv (p_a - p_1)^2 = -\sqrt{s}E_1(1-\cos\theta)\,, \tag{A.10}$$

$$t_2 \equiv t = (p_1 + p_2 - p_a)^2\,, \tag{A.11}$$

$$s_1 \equiv p_c^2 = (p_1 + p_2)^2\,, \tag{A.12}$$

$$s_2 \equiv (p_a + p_b - p_1)^2 = s - 2\sqrt{s}E_1\,. \tag{A.13}$$

We denote the three-body phase space integral by

$$R_3(s) \equiv \int \prod_{i=1}^{3} \frac{d^3p_i}{2E_i}\,\delta^{(3)}(\boldsymbol{p_a} + \boldsymbol{p}_b - \boldsymbol{p}_1 - \boldsymbol{p}_2 - \boldsymbol{p}_3)\,\delta(\sqrt{s} - E_1 - E_2 - E_3)\,. \tag{A.14}$$

The key formula that we need is given by eq. V-7.8 of ref. [104],

$$\frac{dR_3}{ds_2 dt_1 ds_1} = \frac{\pi}{8\lambda^{1/2}(s, m_a^2, m_b^2)\lambda^{1/2}(s, s_2, m_1^2)}\,\Theta\{-G(s, t_1, s_2, m_a^2, m_b^2, m_1^2)\}$$
$$\times\Theta\{-G(s_1, s_2, s, m_2^2, m_1^2, m_3^2)\}\int_0^{2\pi} d\phi\,, \tag{A.15}$$

where $G$ is the basic four-particle kinematic function first introduced in ref. [105,106],

$$G(x,y,z,u,v,w) \equiv -\frac{1}{2}\det\begin{pmatrix} 2u & x+u-v & u+w-y \\ x+u-v & 2x & x-z+w \\ u+w-y & x-z+w & 2w \end{pmatrix}\,, \tag{A.16}$$



JHEP09(2011)027

and $\lambda$ is the triangle function defined in eq. (A.4). Expanding out the determinant yields the unwieldy expression,[11]

$$G(x,y,z,u,v,w) = xy(x+y) + zu(z+u) + vw(v+w) + x(zw+uv) + y(zv+uw) \\ -xy(z+u+v+w) - zu(x+y+v+w) - vw(x+y+z+u)\,. \qquad \text{(A.17)}$$

Finally, $\phi$ is the so-called *helicity angle* [104], which is most conveniently defined in a reference frame where $\vec{\boldsymbol{p}}_2 + \vec{\boldsymbol{p}}_3 = \vec{\boldsymbol{p}}_a + \vec{\boldsymbol{p}}_b - \vec{\boldsymbol{p}}_1 = 0$. In this reference frame, $\phi$ is identified as the azimuthal angle between the production plane spanned by $\vec{\boldsymbol{p}}_b$ and $\vec{\boldsymbol{p}}_1$ and the plane spanned by $\vec{\boldsymbol{p}}_1$ and $\vec{\boldsymbol{p}}_3$, with $\vec{\boldsymbol{p}}_1$ as the axis. The angle $\phi$ can be re-expressed in terms of the Lorentz-invariant variables $s_1$, $s_2$, $t_1$ and $t_2$, as exhibited in eq. V-8.8 of ref. [104]. In particular, it will be convenient to express $t_2$ in terms of $s_1$, $s_2$, $t_1$ and $\cos\phi$ following eq. V-8.9 of ref. [104],

$$m_b^2 + m_3^2 - t_2 = \frac{D - 2\left[G(s,t_1,s_2,m_a^2,m_b^2,m_1^2)G(s_1,s_2,s,m_2^2,m_1^2,m_3^2)\right]^{1/2}\cos\phi}{\lambda(s,s_2,m_1^2)}\,, \qquad \text{(A.18)}$$

where

$$D \equiv \det\begin{pmatrix} 2s & s+s_2-m_1^2 & s-s_1+m_3^2 \\ s+s_2-m_1^2 & 2s_2 & s_2-m_2^2+m_3^2 \\ s-m_a^2+m_b^2 & s_2-t_1+m_b^2 & 0 \end{pmatrix}. \qquad \text{(A.19)}$$

Note that the phase space distribution in the helicity angle is uniform, as the integration over $\phi$ in eq. (A.15) is trivial. However, because the matrix element given in eq. (A.2) depends on $t \equiv t_2$, the calculation of the partonic cross section for $a+b \to 1+2+3$ will require a nontrivial integration over $\phi$.

The step functions in eq. (A.15) determine the kinematical ranges of the parameters $s_1$, $s_2$ and $t_1$. Taking $m_a = m_b = m_1 = 0$ and $m_2 = m_3 = m$, it follows that:

$$\frac{dR_3}{ds_2 dt_1 ds_1} = \frac{\pi}{8s(s-s_2)}\,\Theta\{-G(s,t_1,s_2,0,0,0)\}\Theta\{-G(s_1,s_2,s,m^2,0,m^2)\}\int_0^{2\pi} d\phi\,. \qquad \text{(A.20)}$$

The differential cross-section is given by:

$$d\sigma = \frac{1}{64\pi^5 s} dR_3(s)|\mathcal{M}(a+b\to 1+2+3)|^2\,, \qquad \text{(A.21)}$$

where the squared matrix element is suitably averaged over initial spins and summed over final spins. The dominant contribution to $a+b\to 1+2+3$ takes place via $a+b\to c+3$, where $c$ is produced approximately on-shell and subsequently decays via $c\to 1+2$. In particular, since $c$ is a spin-zero particle,

$$|\mathcal{M}(a+b\to 1+2+3)|^2 \simeq \frac{|\mathcal{M}(a+b\to c+3)|^2\,|\mathcal{M}(c\to 1+2)|^2}{(s_1-M^2)^2+M^2\Gamma^2}\,. \qquad \text{(A.22)}$$

We now use eqs. (A.2) and (A.5) and employ the narrow width approximation,

$$\frac{1}{(s_1-M^2)^2+M^2\Gamma^2} \longrightarrow \frac{\pi}{M\Gamma}\delta(s_1-M^2)\,. \qquad \text{(A.23)}$$

[11] Eq. (A.17), which was first defined in ref. [105,106], is also given in eq. IV-5.23 of ref. [104]. We have noted a typographical error in the latter; in the second line of eq. IV-5.23, the first term $yzw$ should read $yzv$.



JHEP09(2011)027

Hence, it follows that:

$$\frac{d\sigma}{ds_2 dt_1 ds_1} = \frac{B}{32\pi^2 \xi s^2 (s-s_2)} \delta(s_1 - M^2)\Theta\{-G(s,t_1,s_2,0,0,0)\}$$
$$\times\Theta\{-G(s_1,s_2,s,m^2,0,m^2)\}\int_0^{2\pi} |C_1(s,t_2)|^2 d\phi\,, \qquad \text{(A.24)}$$

where $t_2$ should be expressed in terms of $s_1$, $s_2$, $t_1$ and $\cos\phi$ using eq. (A.18) before performing the integration over $\phi$, and

$$\xi \equiv 1 - \frac{m^2}{M^2}\,. \qquad \text{(A.25)}$$

Assuming that $G(s_1,s_2,s,m^2,0,m^2) < 0$, we can immediately use the $\delta$-function to integrate over $s_1$. Using eq. (A.17), we obtain:

$$\begin{aligned} G(s_1,s_2,s,m^2,0,m^2) &= s_1^2 s_2 - s_1 s_2 (s - s_2 + 2m^2) + m^2 s(s-s_2) + s_2 m^4 \\ &= s_2 (s_1 - s_1^+)(s_1 - s_1^-)\,, \end{aligned} \qquad \text{(A.26)}$$

where $s_2$ is strictly non-negative and

$$s_1^\pm = m^2 + \frac{1}{2}(s-s_2)\left[1 \pm \sqrt{1 - \frac{4m^2}{s_2}}\right]\,. \qquad \text{(A.27)}$$

That is, we require that:

$$s_1^- \le M^2 \le s_1^+\,, \qquad \text{(A.28)}$$

otherwise, $s_1 = M^2$ can never be satisfied when $G(s_1,s_2,s,m^2,0,m^2) < 0$. Note that eq. (A.28) yields upper and lower limits for $s_2$. One can then use eq. (A.13) to obtain upper and lower limits for $E_1$. These limits correspond to the roots of the quadratic equation,

$$4\sqrt{s}M^2 E_1^2 - 2(M^2-m^2)(s+M^2-m^2)E_1 + \sqrt{s}(M^2-m^2)^2 = 0\,. \qquad \text{(A.29)}$$

These roots can be expressed as:[12]

$$E_1^\pm \equiv \frac{\xi}{4\sqrt{s}}\left[s + M^2 - m^2 \pm \lambda^{1/2}(s,M^2,m^2)\right]\,, \qquad \text{(A.30)}$$

where $\xi$ is defined in eq. (A.25). Likewise, employing eq. (A.13), we define

$$s_2^\pm = s - 2\sqrt{s}E_1^\mp\,. \qquad \text{(A.31)}$$

The range of $t_1$ is determined from the inequality:

$$G(s,t_1,s_2,0,0,0) \equiv s t_1 (s + t_1 - s_2) \le 0\,, \qquad \text{(A.32)}$$

[12]Note that eq. (A.30) is equivalent to $E_1^\pm = \frac{1}{2}\xi(E_c \pm p_c)$, where $E_c$ and $p_c$ are the center-of-mass energy and momentum of the decaying particle $c$.



JHEP09(2011)027

where we have used eq. (A.17) to evaluate the $G$-function. That is, as $s_2$ ranges over $s_2^- \leq s_2 \leq s_2^+$,

$$s_2 - s \leq t_1 \leq 0\,. \tag{A.33}$$

Assuming that $s_2^- \leq s_2 \leq s_2^+$, the integration of eq. (A.24) over $s_1$ is immediate, and we obtain:

$$\frac{d\sigma}{ds_2 dt_1} = \frac{B}{32\pi^2 \xi s^2 (s-s_2)}\,\Theta\{-G(s,t_1,s_2,0,0,0)\}\int_0^{2\pi} |C_1(s, A_1 + A_2\cos\phi)|^2 d\phi\,, \tag{A.34}$$

where eq. (A.18) has been used to write $t_2 = A_1 + A_2\cos\phi$. Using eqs. (A.26) and (A.32) with $s_1 = M^2$, $m_a = m_b = m_1 = 0$ and $m_2 = m_3 = m$, the coefficients $A_1$ and $A_2$ are given by

$$A_1 = m^2 - \frac{s_2(s-s_2+t_1)(M^2-m^2) - st_1(s-s_2-M^2+m^2)}{(s-s_2)^2}\,, \tag{A.35}$$

$$A_2 = \frac{2\left[st_1(s-s_2+t_1)(M^4 s_2 - M^2 s_2(s-s_2+2m^2) + m^2 s(s-s_2) + s_2 m^4)\right]^{1/2}}{(s-s_2)^2}\,. \tag{A.36}$$

We now introduce the transverse momentum, $p_T$ of particle 1, which is defined by $p_T = E_1 \sin\theta$. Note that

$$st_1(s+t_1-s_2) = -s^2 p_T^2\,, \tag{A.37}$$

which is strictly non-positive as required by eq. (A.32). In particular,

$$\cos\theta = \pm\sqrt{1 - \frac{p_T^2}{E_1^2}}\,, \tag{A.38}$$

where the $\pm$ indicates that $\theta$ and $\pi - \theta$ correspond to the same value of $p_T$. Thus, eq. (A.10) yields

$$t_1 = -\sqrt{s}\left(E_1 \mp \sqrt{E_1^2 - p_T^2}\right)\,. \tag{A.39}$$

One can now perform a change of variables from $\{t_1\,,\, s_2\}$ to $\{p_T^2\,,\, E_1\}$. Computing the Jacobian of the transformation, it follows that:

$$dt_1 ds_2 = \frac{s dp_T^2 dE_1}{\sqrt{E_1^2 - p_T^2}}\,. \tag{A.40}$$

The limits of the kinematic variables $p_T$ and $E_1$ are given by:

$$0 \leq p_T \leq E_1\,, \qquad E_1^- \leq E_1 \leq E_1^+\,, \tag{A.41}$$

where the range of $p_T$ follows from $|\cos\theta| \leq 1$ and $E_1^\pm$ is defined in eq. (A.30). Since we aim to compute $d\sigma/dp_T$, it is more useful to interchange the order of integration. Thus, equivalent to eq. (A.41) is:

$$\text{for}\quad 0 \leq p_T \leq E_1^-\,, \qquad E_1^- \leq E_1 \leq E_1^+\,, \tag{A.42}$$

$$\text{for}\quad E_1^- \leq p_T \leq E_1^+\,, \qquad p_T \leq E_1 \leq E_1^+\,. \tag{A.43}$$



JHEP09(2011)027

Combining eqs. (A.34) and (A.40), and adding the contributions from the two possible values of $t_1$ that yield the same value of $p_T$ [cf. eq. (A.39)], one obtains:

$$\frac{d\sigma}{dp_T^2 dE_1} = \frac{B}{64\pi^2 \xi s^{3/2} E_1 \sqrt{E_1^2 - p_T^2}} \int_0^{2\pi} d\phi \sum_{j=\pm} |C_1(s, A_1^{(j)} + A_2 \cos\phi)|^2 \,, \tag{A.44}$$

where $A_1^{(\pm)}$ is defined by eq. (A.35), and the superscript indicates which sign is used in eq. (A.39) to express $t_1$ in terms of $E_1$ and $p_T^2$. In contrast, $A_2$ [defined in eq. (A.36)] does not depend on the sign choice in eq. (A.39) as a consequence of eq. (A.37).

We now integrate over $E_1$, employing the limits of integration given in eqs. (A.42) and (A.43). Writing $dp_T^2 = 2p_T dp_T$, we arrive at our final result,[13]

$$\frac{d\sigma}{dp_T} = \frac{Bp_T}{32\pi^2 \xi s^{3/2}} \int_{E_{\rm min}}^{E_{\rm max}} \frac{dE_1}{E_1 \sqrt{E_1^2 - p_T^2}} \int_0^{2\pi} d\phi \sum_{j=\pm} |C_1(s, A_1^{(j)} + A_2 \cos\phi)|^2 \,, \tag{A.45}$$

where the upper and lower limits of integration are given by $E_{\rm max} \equiv E_1^+$ and

$$E_{\rm min} = \begin{cases} E_1^- & \text{for } \ 0 \le p_T \le E_1^- \,, \\ p_T & \text{for } \ E_1^- \le p_T \le E_1^+ \,. \end{cases} \tag{A.46}$$

As a warmup, we shall ignore the details of the scattering matrix element for the process $a+b \to c+3$ by putting $C_1 = 1$. In this case, the integrals in eq. (A.45) are elementary, and the end result is:

$$\frac{d\sigma}{dp_T} = \frac{B}{8\pi\xi s^{3/2}} \left[ \tan^{-1}\left( \frac{\sqrt{[E_1^+]^2 - p_T^2}}{p_T} \right) - \Theta(E_1^- - p_T) \tan^{-1}\left( \frac{\sqrt{[E_1^-]^2 - p_T^2}}{p_T} \right) \right] , \tag{A.47}$$

where $0 \le p_T \le E_1^+$, and the step function $\Theta$ is defined as usual,

$$\Theta(E_1^- - p_T) = \begin{cases} 1 & \text{for } \ 0 \le p_T \le E_1^- \,, \\ 0 & \text{for } \ E_1^- \le p_T \le E_1^+ \,. \end{cases} \tag{A.48}$$

It is convenient to introduce dimensionless variables,

$$w \equiv \frac{2E_1}{\sqrt{s}} \,, \qquad x \equiv \frac{2p_T}{\sqrt{s}} \,, \qquad y \equiv \frac{M^2}{s} \,, \qquad z \equiv 1 - \xi = \frac{m^2}{M^2} \,. \tag{A.49}$$

The kinematics of the scattering process requires that $\sqrt{s} \ge M + m$, which is equivalent to the condition,

$$\sqrt{y}\,(1 + \sqrt{z}) \le 1 \,. \tag{A.50}$$

The range $w$ is given by $w^- \le w \le w^+$, where

$$w^\pm = \frac{1}{2}(1-z)\left[ 1 + y(1-z) \pm \lambda^{1/2}(1, y, yz) \right] \,. \tag{A.51}$$

[13] There is no singularity in the limit of $\xi \to 0$ since in this limit, $E^\pm \to 0$.



JHEP09(2011)027

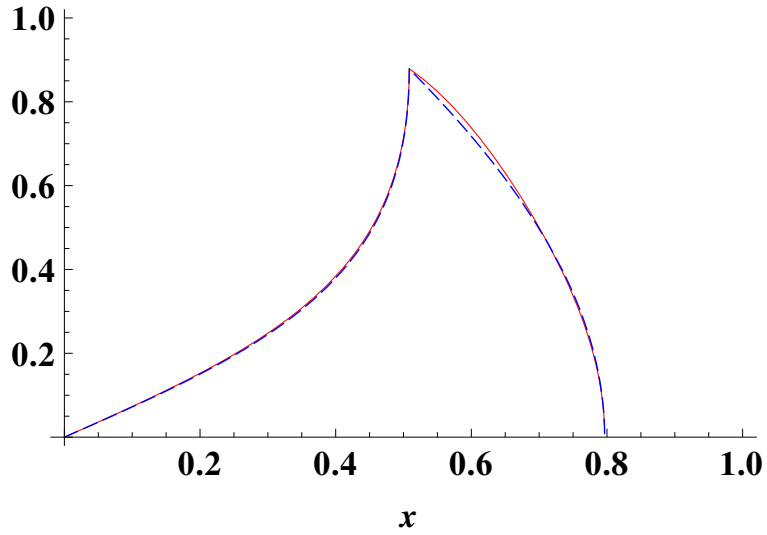


**Figure 10**. Unnormalized $p_T$ distributions for $a+b \to c+3$, $c \to 1+2$, assuming that the matrix element for $a+b \to c+3$ is constant (dashed curve) or is given by eq. (A.54) (solid curve). The rescaled transverse momentum is defined by $x \equiv 2p_T/\sqrt{s}$ and can take on values in the range $0 \le x \le x_{\rm max}$, where $x_{\rm max} \equiv \frac{1}{2}(1-z)\left[1+y(1-z)+\lambda^{1/2}(1,y,yz)\right]$. The masses of particles $c$ and $d$ are fixed by $y \equiv M^2/s = 0.5$ and $z \equiv m^2/M^2 = 0.1$. To facilitate the comparison of the two $p_T$ distributions, the relative normalization of the two curves has been fixed such that the height of the peaks of the distributions coincide. The *location* of the peak at $x = 0.50843$, corresponding to eq. (A.53), is the same for both curves.

Hence, the range of $x$ is

$$0 \le x \le w^+ < 1\,. \tag{A.52}$$

As an example, take $y = 0.5$ and $z = 0.1$, which is consistent with the inequality given in eq. (A.50). Eq. (A.52) then implies that $0 \le x \le 0.79657$. The transverse momentum distribution, plotted in figure 10 exhibits a striking Jacobian peak located at $x = 0.50843$, which corresponds to

$$(p_T)_{\rm peak} = E_1^-\,. \tag{A.53}$$

The origin of the Jacobian peak is a consequence of the change in kinematic variables given in eq. (A.40), and is rather insensitive to the form of the matrix element. To illustrate this point, we have numerically evaluated eq. (A.45), where the tree-level form for $C_1$ for $gq \to \widetilde{q}_R\widetilde{\chi}_1^0$ is employed [11, 35, 36, 62]

$$|C_1(s,t)|^2 = N\left[\frac{s+t-M^2}{2s} - \frac{M^2(m^2-t)}{(M^2-t)^2} + \frac{sm^2+(m^2-t)(M^2-m^2)}{s(M^2-t)}\right], \tag{A.54}$$

where $N$ is an overall dimensionless normalization factor that depends on the relevant couplings. In terms of the dimensionless variables introduced in eq. (A.49),

$$\frac{d\sigma}{dx} = \frac{Bx}{64\pi^2 s(1-z)}\int_{w_{\rm min}}^{w_{\rm max}}\frac{dw}{w}\frac{1}{\sqrt{w^2-x^2}}\int_0^{2\pi}d\phi\sum_{j=\pm}|C_1(s,A_1^{(j)}+A_2\cos\phi)|^2\,, \tag{A.55}$$



JHEP09(2011)027

where

$$w_{\max} = w^+ \,, \qquad w_{\min} = \begin{cases} w^- \,, & \text{for } 0 \le x \le w^- \,, \\ x \,, & \text{for } w^- \le x \le w^+ \,, \end{cases} \tag{A.56}$$

and the coefficients $A_1^{(\pm)}$ and $A_2$ are given by:

$$A_1^{(\pm)} = \frac{1}{2} s \left\{ y(1+z) - 1 \pm \frac{\sqrt{w^2 - x^2}\,[w + y(1-z)(w-2)]}{w^2} \right\}, \tag{A.57}$$

$$A_2 = \frac{sxy^{1/2}}{w^2} \left[ w(1-w-z) - y(1-w)(1-z)^2 \right]^{1/2} . \tag{A.58}$$

The resulting unnormalized $p_T$ distribution is exhibited in figure 10. Note that the shape of the $p_T$ distribution is dominated by the explicit kinematic factors that appear in eq. (A.45), and depends quite weakly on the actual form of the squared-matrix element given in eq. (A.54). Moreover, the location of the peak in the $p_T$ distribution is unchanged and given by eq. (A.53), as a consequence of structure of the kinematic limits given in eqs. (A.42) and (A.43).

In the above analysis, the location of the Jacobian peak given in eq. (A.53) depends on the partonic center-of-mass energy $\sqrt{s}$. The differential cross section for the hadronic scattering process, $A + B \to c + 3 + X \to 1 + 2 + 3 + X$, is obtained by convoluting the $p_T$ distribution of the partonic subprocess, $a + b \to c + 3 \to 1 + 2 + 3$, with the product of the parton distribution functions $f_a^A(x_1, Q^2) f_b^B(x_2, Q^2)$, where the total center-of-mass squared-energy $S$ is related to the partonic center-of-mass energy via $s = x_1 x_2 S$, and $Q$ is the factorization scale. In the convolution, partonic center-of-mass energies close to the energy threshold for the partonic process provide the dominant contribution to the production of the final state. In this case, one can derive an approximate formula for the location of the Jacobian peak that does not depend on the partonic center of mass energy. The threshold for $a + b \to c + 3$ corresponds to the point at which

$$\lambda(s, M^2, m^2) = (s + M^2 - m^2)^2 - 4sM^2 = 0 \,. \tag{A.59}$$

At this point $s + M^2 - m^2 = 2M\sqrt{s}$ (or equivalently, $\sqrt{s} = M + m$), in which case

$$E_1^- = E_1^+ = \frac{M^2 - m^2}{2M} \,. \tag{A.60}$$

Of course, the cross-section given in eq. (A.45) vanishes exactly at threshold where $E_1^- = E_1^+$. However, if we are close to threshold, then eq. (A.60) still provides a decent approximation to $E_1^-$, in which case the location of the Jacobian peak is:

$$(p_T)_{\text{peak}} = E_1^- \simeq \frac{M^2 - m^2}{2M} = \frac{1}{2} \xi M \,, \tag{A.61}$$

which is independent of the partonic center-of-mass energy.

In this paper, we have numerically computed the transverse momentum distribution of the hadronic scattering process, taking into account the partonic scattering process at all



JHEP09(2011)027

allowed values of the partonic center-of-mass energy. In particular, as the partonic center-of-mass energy is increased above the threshold energy for $a+b \to c+3$, the location of the peak of the partonic transverse momentum distribution, $E_1^-$ [cf. eq. (A.30)] *decreases* relative to the estimate given in eq. (A.61). Thus, we expect the actual peak in the transverse momentum distribution of the hadronic scattering process (or equivalently in the missing transverse energy distribution) to be somewhat less than the result of eq. (A.61). This is indeed the case in the $\not{p}_T$ distributions that we exhibit in this paper.

Note that in the approximation that the transverse momentum of particle $c$ is due entirely from the hard scattering process (i.e. the transverse momentum of the initial partons and the spectators are neglected), the distribution of the missing transverse energy (i.e. particles 2 and 3 of the hard scattering process) should precisely match that of the transverse momentum of the monojet (i.e. particle 1 of the hard scattering process). Of course, the effects of spectators, initial and final state radiation, fragmentation of final state partons, jet mismeasurements and detector effects will tend to reduce the sharpness of the peak in the $\not{p}_T$ distributions as compared to that of figure 10.

JHEP09(2011)027